SUPPORTING INFORMATION TO

Interaction of Atomic Hydrogen with the Cu_2O(100) and (111) Surfaces

Heloise Tissot[1], Chunlei Wang[1], Joakim Halldin Stenlid[2], Mohammad Panahi[4], Sarp Kaya[4,5], Milad Ghadami Yazdi[1], Markus Soldemo[1], Tore Brinck[3], Jonas Weissenrieder[1]

[1] Material Physics, School of Engineering Sciences, KTH Royal Institute of Technology, SE-100 44 Stockholm, Sweden

[2] Department of Physics, Albanova University Center, Stockholm University, SE-106 91, Stockholm, Sweden

[3] Applied Physical Chemistry, Department of Chemistry,

KTH Royal Institute of Technology, SE-100 44 Stockholm, Sweden

[4] Material Science and Engineering, Koç University, Istanbul, Turkey

[5] Chemistry Department, Koç University, Istanbul, Turkey

- Cu_2O(100) surface after exposure to atomic hydrogen: STS measurements

STS measurements were performed on the (3,0;1,1)-Cu_2O(100) surface after exposure to atomic hydrogen for 1 min ($P(H_2) = 2 \times 10^{-8}$ mbar, emission current = 30 mA) STS was performed on the clean rows and on the bright protrusions formed after atomic hydrogen adsorption, none of the protrusions show any states in the band gap as was observed for defects such as oxygen vacancies (refs 27 and 28 of the main article). This observation confirms that in the present case, the protrusions are due to OH groups created after the reaction of hydrogen atoms with surface oxygen atoms.

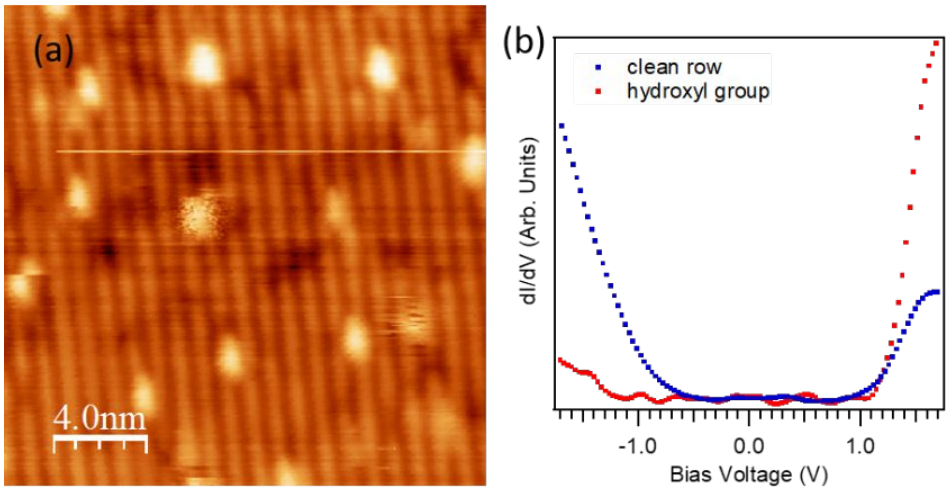

Figure S1: a) STM images of the $Cu_2O(100)$ surface after exposure to atomic hydrogen ($P(H_2)$ = 2×10^{-8} mbar, Emission current = 30 mA, 1 min), b) STS curve measured on a surface hydroxyl group.

- $Cu_2O(100)$ surface after exposure to water

The OH coverage obtained for high dosage of atomic hydrogen (saturated surface) can be compared to the coverage obtained after water adsorption on the same surface. To saturate the surface with hydroxyl groups, water is adsorbed at low temperature (~100 K) in order to form a dense ice layer on the surface. The surface is then annealed to desorb the bulk ice. The spectrum presented here is recorded at 180 K. The binding energy position of the OH groups is 531.3 eV and the ratio OH / O_B is 0.25.

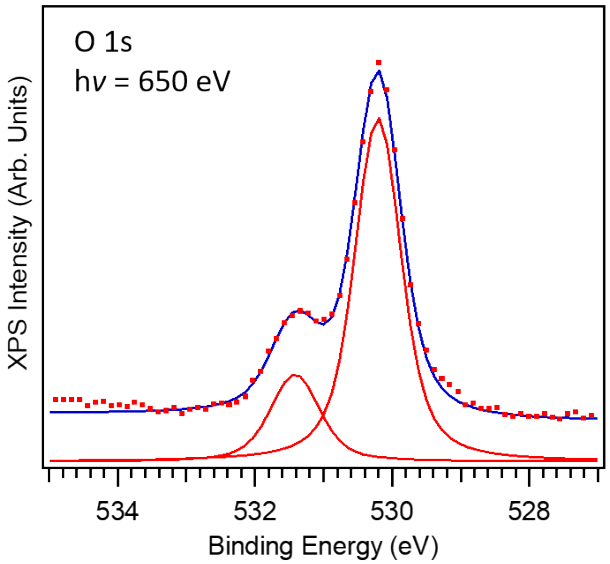

Figure S2: O 1s XPS spectra after exposure of the clean $Cu_2O(100)$ surface to water at 100 K followed by annealing to 180 K.

- $Cu_2O(100)$ surface after 3 cycles of exposure to atomic hydrogen and annealing at 475 K: XPS data

Figure S3 presents the O 1s and C1s spectra from the $Cu_2O(100)$ surface after 3 cycles of exposure to atomic hydrogen ($P(H_2) = 2 \times 10^{-8}$ mbar, emission current = 40 mA, 2 min) and annealing at 475 K. In the O 1s spectra, the main peak at 530.2 eV is associated to oxygen atoms in the bulk lattice of Cu_2O (O_B) and the shoulder at lower energy is attributed to surface oxygen atoms (surface (S2) and first layer of subsurface (S1) oxygen atoms). The presence of this shoulder can be considered as a fingerprint for the clean (3,0;1,1) reconstructed surface. However, no additional peak at higher binding energy that could be assigned to OH groups on the surface are observed. These two observations confirm the removal of OH groups from the surface after annealing and the reconstruction of the surface. The C 1s region is also presented to demonstrate the absence of carbon contaminants on the sample surface after exposure to atomic hydrogen.

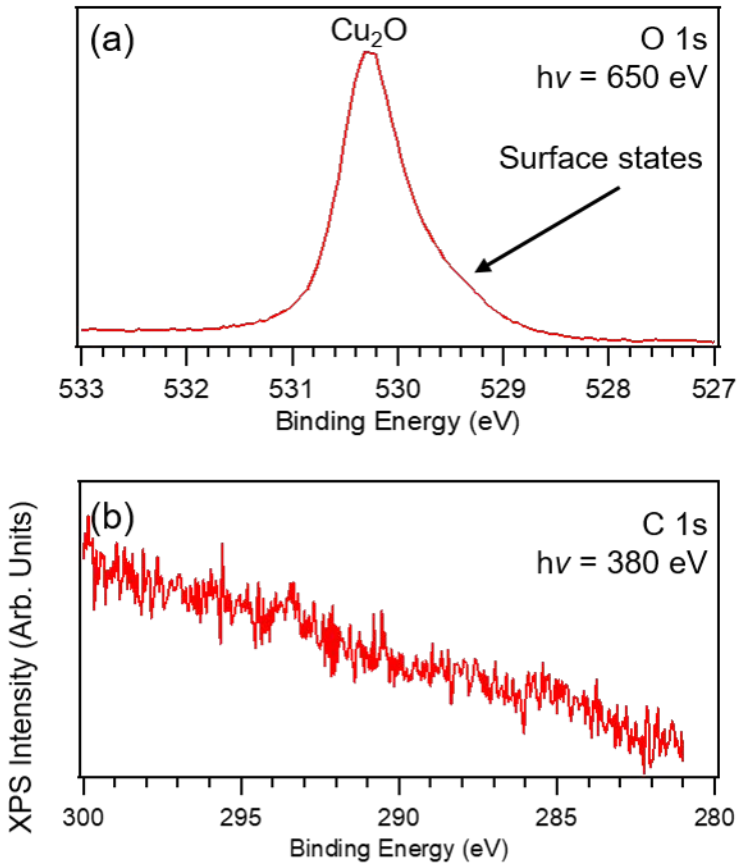

Figure S3: (a) O 1s and (b) C 1s XPS of the $Cu_2O(100)$ surface after 3 cycles of exposure to atomic hydrogen ($P(H_2) = 2 \times 10^{-8}$ mbar, emission current = 40 mA, 2 min) and annealing at 475 K.

- $Cu_2O(111)$ surface after exposure to atomic hydrogen:

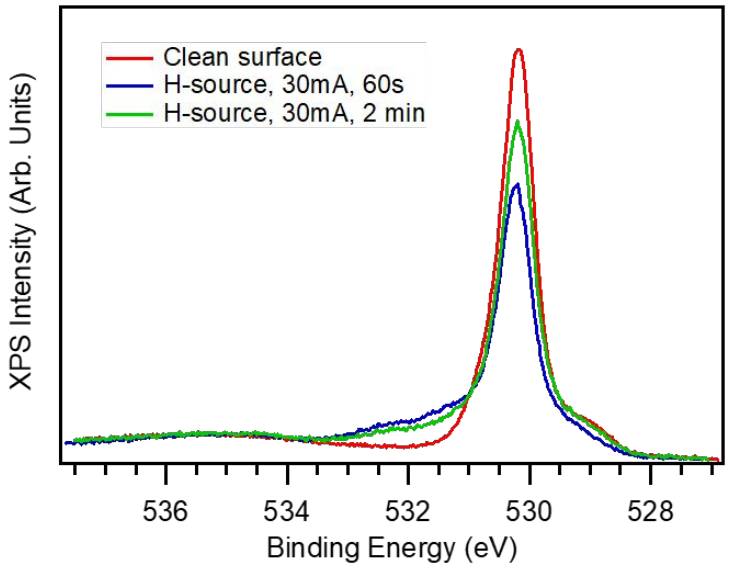

Figure S4: O 1s XPS spectra after exposure of the clean $Cu_2O(111)$ surface to atomic hydrogen. All spectra were collected with a photon energy of 650 eV.

Unlike what was observed for the $Cu_2O(100)$ surface, the S component does not disappear completely during atomic hydrogen exposure. Figure S4 shows a decrease of component S and also of O bulk species suggesting that oxygen atoms forming hydroxyl groups also come from subsurface positions.

- Effect of annealing in CO TPD from atomic hydrogen dosed $Cu_2O(100)$ surface

The annealing temperature is critical since metallic copper clusters can diffuse readily at elevated temperature. Migration of oxygen ions from the bulk is another thermally activated facile process. CO adsorption, that is sensitive to the chemical nature of the surface sites, can thus be influenced by the thermal treatment of the modified surface. As CO TPD traces clearly indicate, desorption profile changes with increasing temperature, traces begin to resemble to CO TPD from clean Cu(100) above 700 K, indicating that the surface is recovering.

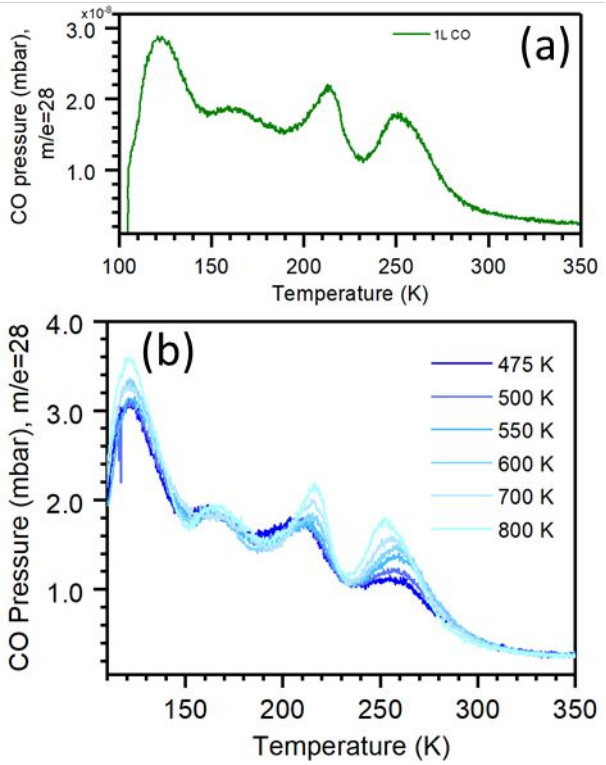

Figure S5: TPD traces after adsorption of 1 L CO at 100 K on (a) the clean $Cu_2O(100)$ surface and (b) after annealing the atomic hydrogen dosed (3×5 min) $Cu_2O(100)$ surface to the respected temperatures.

- Density functional theory results:

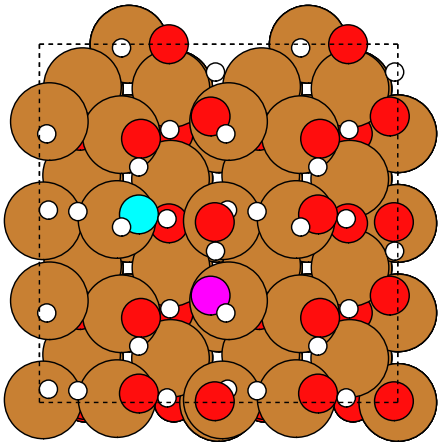

Figure S6: Low-energy mixed H_2O/OH/H adsorption layer structure on (1 × 1)/c(2 × 2) reconstructed $Cu_2O(100)$ as determined by Stenlid et al. (ref 26 of main article). The cyan O of a H_2O molecule has a computed O 1s surface core level shift (SCLS) of 1.87 eV towards higher

binding energy relative to bulk O, and the magenta O in OH has a SCLS of 0.81 eV. The shifts are computed according to the procedures of Soldemo et al. (ref 23 of main article).

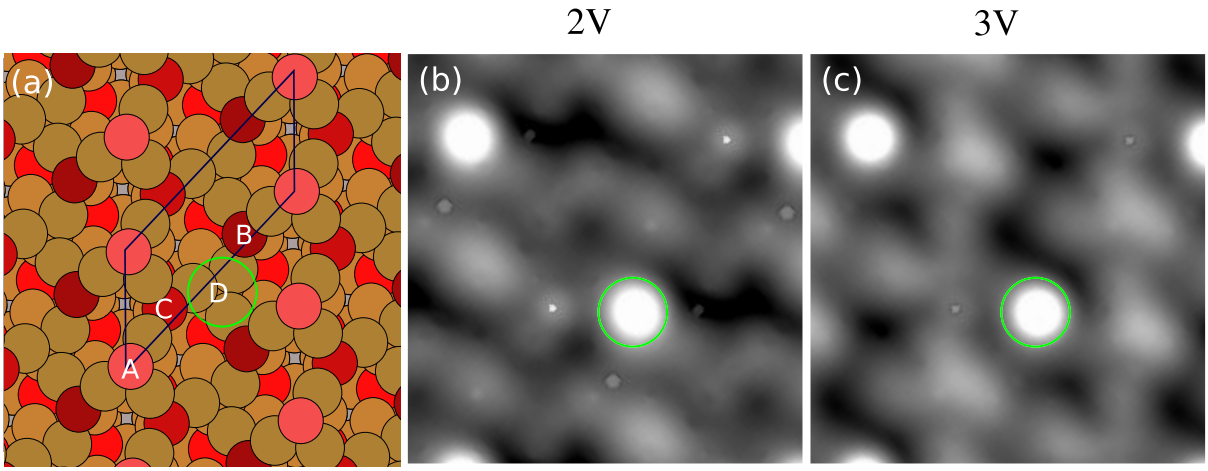

Figure S7: (a) atomic model of $Cu_2O(100)$:(3,0;1,1) with marked sites. Simulated STM images for the D' H adsorption mode, i.e. OH_{ad} at the D site after migration from the B site, for different bias voltages in (b) and (c) computed according to the procedures specified in ref 23 of the main article.

Table S1. Adsorption positions and adsorption energies (ΔE_{ad}) relative the most favored site in eV on the $(\sqrt{3} \times \sqrt{3})R30°$ reconstructed $Cu_2O(111)$ surface. (Purple balls represent lattice oxygen atoms, dark red O_{CUS} atoms, and bright red subsurface O atoms. Brown balls are copper atoms where dark brown depicts Cu_{CUS}).

Cu vacancies	**Location**	**ΔE_{ad}**
No	O_{CUS}	0.22
No	Cu_{CUS}	0.00
No	O^{VAC}	0.36
Yes	O_{CUS}	0.36
Yes	O^{VAC}	0.00

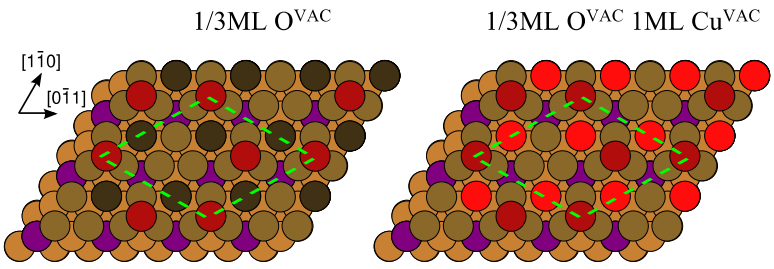

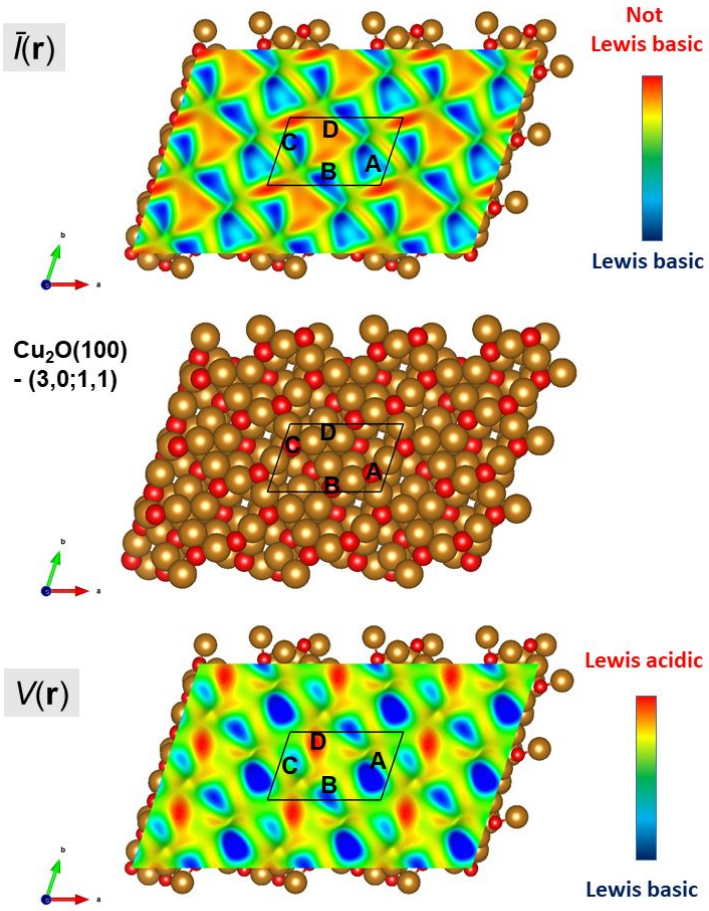

Figure S8: Showing the local properties $V(\mathbf{r})$ (bottom) and $\bar{I}(\mathbf{r})$ (top) plotted on the 0.001 au isodensity contour of the (3,0;1,1) reconstructed $Cu_2O(100)$ surface (atomic model in middle). $V(\mathbf{r})$ and $\bar{I}(\mathbf{r})$ are defined below by eq. 1 and 2, respectively. $V(\mathbf{r})$ indicates sites that are acidic (red > yellow) and basic (blue > cyan), and reflect the site's susceptibility to electrostatic interactions. The $V(\mathbf{r})$ property ranks the basicity of the sites as A > B > C corresponding to the magnitude of their local minima in the surface $V(\mathbf{r})$ ($\Delta V_{S,min}$, values versus site C: -0.5 eV and -0.2 eV for A and B, respectively), whereas the D site is indicated as acidic with a local positive $V_S(\mathbf{r})$. For the $\bar{I}_S(\mathbf{r})$ property the lowest, most favorable ionization energy is found at the A and B sites. They have the same $\bar{I}_{S,min}$ of -11.4 eV, while the C site is less basic with an $\bar{I}_{S,min}$ of -11.3 eV. This suggests that the A and B site have the same intrinsic basicity when also the charge-transfer capacity is accounted for. We also note that in order to capture the full basicity of the sites, also effects such as structure relaxation should be accounted for.

In the equation of the electrostatic potential below, Z_A and $\mathbf{R}_A$ are the charge and position of the A^{th} nucleus. The positions of the electrons are given by $\mathbf{r}$ and the electron (charge) density by $\rho(\mathbf{r})$. The potential is corrected to absolute scale by comparing to the local potential at the middle of the vacuum region of the slab model.

$$V(\mathbf{r}) = \sum_A \frac{Z_A}{|\mathbf{R}_A - \mathbf{r}|} - \int \frac{\rho(\mathbf{r}')d\mathbf{r}'}{|\mathbf{r}' - \mathbf{r}|} - V_{\text{vac}}^{\text{per}} \quad \text{(eq. 1)}$$

The average local ionization energy $\bar{I}(\mathbf{r})$ is defined by equation 2 below. In the equation, $\rho_{\text{i,k}}(\mathbf{r})$ is the charge density function of the i^{th} state of **k**-point k, where contributions are summed over all **k**-points n_{kpts} and all occupied states up to the fermi level E_{F}. The $\rho(\mathbf{r})$ is the total charge density, $\varepsilon_{\text{i,k}}$ the eigenvalue of the i^{th} state and ω_{k} a symmetry weighting factor for each **k**-point. E_{vac}^{per} is the vacuum energy of a free electron. This is zero on the absolute scale, but shifted in a periodic calculation why we compare the energy to the vacuum potential at the middle of the slab model (*cf.* $V(\mathbf{r})$ as $E_{\text{vac}}^{per} = V_{\text{vac}}^{\text{per}}$ for a test charge of -1, i.e. the electron charge in atomic units).

$$\bar{I}(\mathbf{r}) = -\sum_{\text{k}=1}^{n_{\text{kpt}}} \sum_{i=1}^{E_F} \frac{w_{\text{k}}(\varepsilon_{i,k} - E_{\text{vac}}^{per})\rho_{i,k}(\mathbf{r})}{\rho(\mathbf{r})} \quad \text{(eq. 2)}$$